Electron distribution function in an electron-beam plasma

V.S. Malinovsky, A.E. Belikov, O.V. Kuznetsov, and R.G. Scharafutdinov
Institute of Thermophysics, Russian Academy of Sciences, Novosibirsk, 630090, Russia
(Received 28 March 1994; revised manuscript received 12 October 1994)

The spatial energy distribution function of secondary electrons in an electron-beam plasma is studied via a solution of the Boltzmann equation written in the integral form. It is shown that the electron energy distribution function essentially depends on the distance from the center of a primary beam, even with a homogeneous density of a gas medium. Good agreement between the theoretical predictions of the spatial dependence of the electron distribution function and experimental data has been obtained.
PACS number(s): 52.40.Mj, 34.80.Gs, 34.80.Dp

I. INTRODUCTION

The electron distribution function (EDF) under different conditions is the research subject of a large number of studies. Several approaches for determination of the EDF exist [1, 2]. Monte Carlo methods and methods based on the Boltzmann equation are used most often in papers. Traditionally the Boltzmann equation was applied for the determination of the EDF in discharge plasma [3] as well as in electron-beam plasma [2, 4] under quasistationary homogeneous conditions. In this case the EDF is determined averaged over the space [2–4]. Thus the information on the spatial structure of the distribution function is lost. A spatial distribution of electrons is an important characteristic for the diagnostics of flows and jets of low density, in studies of the phenomena of atmospheric physics, and in studies of the processes of the deposition of thin films from gas mixtures when the electron beam is used for excitation. In the electron-beam plasma with the aim of the determination of the EDF as a function of electron energy and position traditionally the Monte Carlo method has been used [1, 5, 6]. The Boltzmann equation has been applied more rarely for the same purpose [7]. Evidently, this situation connects with the simplicity of modeling using the Monte Carlo method. However, the employment of the Boltzmann equation has its own advantages. In particular, there is a possibility to perform qualitative analysis if we have an opportunity to get any analytical expressions.

The purpose of the present paper is to study the spatial energy distribution of electrons generated by a high-energy electron beam passing through a gas medium. The Boltzmann equation for the EDF written in the integral form is employed. The equation takes into account the energy spectrum of secondary electron generation under gas ionization, their escape from the generation region, and energy degradation under activation of molecules (atoms). Calculations are performed up to the first excitation threshold. Electron-electron and electron-ion collisions, multistage ionization, and superelastic collisions were neglected. In addition, electron energy losses under elastic scattering on molecules were ignored. These assumptions are rather justified for the range of electron energies under consideration in the case of weakly ionized plasma, and low pressure electron-beam plasma is exactly this case.

II. BOLTZMANN EQUATION FOR SECONDARY ELECTRONS

In this paper we consider the passage of the electron beam through the gas mixture of spatially homogeneous density. To determine the steady-state distribution function of electrons generated by the electron beam in a gas, we employ the integral Boltzmann equation [7, 8] which, if extended to the case of a gas mixture, takes the form

$$f(\vec{r},e)=\int_V \frac{d^3\vec{r}'}{4\pi}\frac{\exp\left\{-\sum_k \sigma_t^k n_g^k\,|\vec{r}-\vec{r}'|\right\}}{|\vec{r}-\vec{r}'|^2}$$
$$\times\sum_k n_g^k\left\{m_e v_b n_b(\vec{r}')g^k(E,e)\sigma_i^k(E)+\sigma_{\rm el}^k(e)f(\vec{r}',e)+\sum_j \sigma_j^k(e+\Delta e_j)f(\vec{r}',e+\Delta e_j)\right.$$
$$\left.+\int_{e+I_k}^{2e+I_k} d\varepsilon\,\sigma_i^k(\varepsilon)g^k(\varepsilon,\varepsilon-I_k-e)f(\vec{r}',\varepsilon)+\int_{2e+I_k}^{(E-I_k)/2} d\varepsilon\,\sigma_i^k(\varepsilon)g^k(\varepsilon,e)f(\vec{r}',\varepsilon)\right\}, \quad (1)$$

where n_g^k is the density of the kth component of the gas mixture, $\sigma_{\rm el}(e)$ is the momentum-transfer cross section of electron scattering on gas molecules, $\sigma_i(e)$ is the ionization cross section, $\sigma_j(e+\Delta e_j)$ is the inelastic cross section with the energy loss Δe_j by excitation, $\sigma_t(e)$ is the total scattering cross section, $g(e,e')$ is the spectrum of secondary electron generation, I is the ionization energy of the gas molecules, m_e is an electron mass, v_b is the velocity of primary electrons of the beam, E is the energy of primary electrons, and $n_b(\vec{r})$ is the spatial shape of the primary electron beam which was considered monoenergetic.

The steady-state distribution function $f(\vec{r},e)$ specifies the number of the secondary electrons per unit volume in unit velocity interval, i.e., $f(\vec{r},e)$ is normalized by

$$n_e(\vec{r}) = \int dv f(\vec{r},e),$$

where $n_e(\vec{r})$ is the density of the secondary electron.

Equation (1) is written on the assumption of isotropic angular dependence of electron scattering cross sections in different processes. The elastic cross section is replaced by the momentum transfer cross section. The differential scattering cross section for the kth scattering process $\sigma_k(e,\phi)$ is replaced by $\sigma_k(e)/4\pi$, where $\sigma_k(e)$ is the integrated cross section for the kth inelastic process.The abandonment of this assumption would lead to the essential complication of Eq. (1) and the subsequent solution.

The isotropic scattering model is used most in studies [2–4, 6, 7, 9]. The question concerning applicability of this model remains open if the model does not determine the limits of validity. However, in the case in which the scattering is not strongly dependent on the angle we can make the approximation of isotropic scattering. In addition, we are going to examine the suggested model by means of comparison between the theoretical results and results of experiment. We can confirm that the isotropic model is not unreasonable, at least from the point of view of qualitative description of realistic phenomena, if the results of comparison are successful.

Thus we consider the interaction of the electron beam with the gas in the framework of the isotropic scattering model. The following equation for the Bessel transform of the EDF can easily be obtained from Eq. (1) (see Appendix) for a cylindrically symmetric electron beam:

$$\tilde{\varrho}(x,e) = \frac{1}{x}\arctan\left(\frac{x}{\sum_k N_g^k \tilde{\sigma}_t^k(e)}\right)\sum_k N_g^k\left\{g^k(E,e)\,\tilde{\sigma}_t^k(E) + \tilde{\sigma}_{\rm el}^k(e)\,\tilde{\varrho}(x,e) + \sum_j \tilde{\sigma}_j^k(e+\Delta e_j)\,\tilde{\varrho}(x,e+\Delta e_j)\right.$$
$$\left. + \int_{e+I_k}^{2e+I_k} d\varepsilon\,\tilde{\sigma}_i^k(\varepsilon) g^k(\varepsilon,\varepsilon-I_k-e)\,\tilde{\varrho}(x,\varepsilon) + \int_{2e+I_k}^{(E-I_k)/2} d\varepsilon\,\tilde{\sigma}_i^k(\varepsilon) g^k(\varepsilon,e)\,\tilde{\varrho}(x,\varepsilon)\right\}, \quad (2)$$

where

$$\tilde{\varrho}(x,e) = \frac{\varrho(x,e)}{m_e v_b \omega(\nu)}, \quad \tilde{\sigma}_{i,j,{\rm el}} = \frac{\sigma_{i,j,{\rm el}}}{\sigma^*},$$
$$x = \frac{\nu r_0}{\sum_k n_g^k \sigma^* r_0}, \quad N_g^k = \frac{n_g}{\sum_k n_g^k},$$
$$\varrho(x,e) = \int_0^\infty dr\, r J_0(\nu r) f(r,e),$$
$$\omega(\nu) = \int_0^\infty dr\, r J_0(\nu r) n_b(r),$$

$\sigma^* = 1$ Å^2, r_0 is the electron-beam radius, and $J_0(\nu r)$ is the Bessel function of zeroth order.

Equation (2) may be solved in the following way. Taking into account that there are no electrons with the energy exceeding that of primary electrons, and considering the electron generated as a result of ionization of the k molecule by the electron with the energy e as a secondary electron if its energy is $e_1 \le (e-I_k)/2$, we find $\tilde{\varrho}(x,e_{\max})$ from (2), where $e_{\max} = (E-I_k)/2$. Then we add $\tilde{\varrho}(x,e_{\max})$ to the first term in Eq. (2), and find $\tilde{\varrho}(x,e)$ for lesser energy values. Performing the inverse Bessel transformation, we obtain the final expression for the EDF.

III. THE EDF AND EXCITATION RATES

As to understanding of physical processes occurring upon collisions of electrons and molecules, nitrogen appears to be the best-studied system. This is one of the reasons for which it has been chosen as the subject of investigation. In our calculations we employed the following data on the cross sections of N_2: the ionization cross section [10], the electronic excitation cross sections [11], and the momentum-transfer cross section [12]. The generation spectrum of secondary electrons is taken from Ref. [13].

To analyze the EDF, it is also necessary to choose the spatial shape of the primary electron beam. Choosing it Gaussian and taking into consideration that the total number of electrons in the beam is specified by the beam current J and velocity of electrons v_b, for the Bessel transform $\omega(\nu)$ we get

$$\omega(\nu) = \frac{J}{2\pi q_e v_b}\exp\left\{-\nu^2 r_0^2/4\right\}, \quad (3)$$

where q_e is the electron charge.

Using expression (3), for the EDF we obtain

$$f(r,e) = \frac{Jm_e\alpha^2}{2\pi q_e r_0^2}\int_0^\infty dx\, xJ_0(x\alpha r/r_0) \times \exp\{-x^2\alpha^2/4\}\,\tilde{\varrho}\,(x,e)\,, \quad (4)$$

where $\alpha = \sum_k n_g^k \sigma^* r_0$.

Figures 1 and 2 show the energy dependence of the EDF at different distances from the center of the primary electron beam at the densities of nitrogen 10^{16} cm^{-3} and 10^{15} cm^{-3}. It is seen that at short distances from the center of the beam the form of the energy dependence remains practically unchanged. However, at long distances ($r = 10r_0$) essential differences are observed. In particular, at $n_g = 10^{16}$ cm^{-3} the secondary electron density in the energy interval from e_1 to $e_1 + de$ within the range 100 eV $\leq e_1 \leq$1 keV becomes the same (Fig. 1). This result shows that even at homogeneous density of the gas medium the energy dependence of the EDF can vary at different spatial points. Thus the use of the EDF determined from the Boltzmann equation under spatially homogeneous conditions [2–4] may lead to incorrect results, for example, in interpreting experiments on electron-beam plasma diagnostics.

The excitation rate of the jth electronic state of k molecules is defined as

$$F_j(r) = n_g^k \int_0^\infty dv\, v\sigma_j(e) f(r,e)\,, \quad (5)$$

where $\sigma_j(e)$ is the excitation cross section of the jth electronic state, the cross section of ionization or dissociation of a molecule.

The spectral function $\tilde{\varrho}\,(x,e)$ allows one to calculate the spatial profile of the excitation rate of a molecule by secondary electrons without calculating the explicit form of the EDF. Substituting (4) into (5) yields

$$F_j(r) = \frac{n_g^k \sigma^* v_b \alpha^2}{r_0^2}\int_0^\infty dx\, xJ_0(x\alpha r/r_0)\omega(x)\,\tilde{F}_j\,(x)\,, \quad (6)$$

where $\tilde{F}_j\,(x) = \int de\,\tilde{\sigma}_j\,(e)\,\tilde{\varrho}\,(x,e)$.

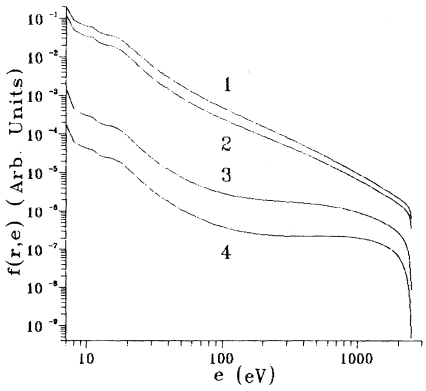

FIG. 1. The energy dependence of the EDF at different distances from the center of the primary electron beam. 1, r = 0; 2, $r = r_0$; 3, $r = 5r_0$; 4, $r = 10r_0$. The gas density $n_g = 10^{16}$ cm^{-3}, the energy of electrons in the beam $E = 5$ keV, the electron-beam radius $r_0 = 5$ mm.

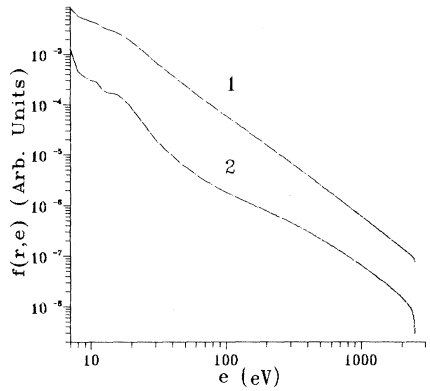

FIG. 2. The energy dependence of the EDF at different distances from the center of the primary electron beam. 1, r = 0; 2, $r = 10r_0$. The gas density $n_g = 10^{15}$cm^{-3}, the energy of electrons in the beam $E = 5$ keV, the electron-beam radius $r_0 = 5$ mm.

The spatial dependence $F_j(r)$ provides important initial information which can serve as a basis for the calculation of the kinetics of excited particles and for the determination of plasma composition. Besides, there is a possibility of comparing the calculated dependence $F_j(r)$ with experimental data on the spatial dependence of radiation intensity of short lifetime states of molecules when the gas motion does not affect measurements.

IV. EXPERIMENT

The above model of the interaction between the electron beam and a gas has been tested by comparing the excitation rate profiles of the state $B\,^2\Sigma_u^+$ of the nitrogen ion and the state $C\,^3\Pi_u$ of the nitrogen molecule with radiation profiles of the first negative (the transition $B\,^2\Sigma_u^+ \rightarrow X\,^2\Sigma_g^+$) and the second positive (the transition $C\,^3\Pi_u \rightarrow B\,^3\Pi_g$) nitrogen systems. This choice is determined by the fact that the states $B\,^2\Sigma_u^+$ and $C\,^3\Pi_u$ are excited in electron-beam plasma by direct electron impact [7] and have short lifetimes.

Experiments have been carried out on the gas dynamics setup of low density [14]. The vacuum chamber of the volume $\sim$ 10 m^3 was pumped by oil pumps of the total capacity 35 m^3/s. The measurements were taken under quasistationary conditions with the gas flow being insignificant. All measurements were performed at gas temperature $T = 298$ K. Pressure was measured by an ionization converter with the error not exceeding 20%. The electron beam of the diameter $\sim$ 3 mm was generated by an electron gun with electromagnetic lens and deflection system. The energy of electrons was $E = 5.5$ keV, the current $i = 5$ mA.

The electron-induced fluorescence was simultaneously detected by the monochromator (the wavelength range 2000–8000 Å, the value of the inverse linear dispersion $D = 6.5$ Å/mm) and x-ray detector measuring the intensity of continuous and characteristic x-ray radiation with the energy of photons $\mathcal{E} \geq 4$ keV. The aperture

of the x-ray detector was limited by a collimator with rectangular cross section. The axis of the collimator and optical axis of the monochromator were perpendicular to the electron-beam axis. The size of the collimator in the direction perpendicular to the electron beam was $l = 2$ mm. Optical radiation was collected to the monochromator by a lens with the focus distance 290 mm and the diameter 100 mm. The half-width and height of the monochromator slit were $\delta = 0.1$ mm and $h = 10$ mm, respectively. The x-ray detector and spectrometer were installed on coordinate mechanisms which allowed us to measure the profile of radiation excited by the electron beam.

V. COMPARISON WITH EXPERIMENT AND CONCLUSIONS

According to the above procedure of measuring radiation intensity, the comparison with experiment requires that the complete excitation rate

$$F_j^t(r) = F_j(r) + F_j^p(r)$$

must be averaged over the observation region. $F_j^p(r)$ denotes the contribution of primary electrons. In the case of a monoenergetic electron beam of the Gaussian shape, the contribution of primary electrons to excitation is defined by the expression

$$F_j^p(r) = \frac{n_g^k \sigma^* J}{\pi q_e r_0^2} \sigma_j(E) \exp\left\{-r^2/r_0^2\right\} .$$

Substituting (3) into expression (6) for the rate of excitation of the jth state by secondary electrons, we obtain

$$F_j(r) = \frac{n_g^k \sigma^* J \alpha^2}{2\pi q_e r_0^2} \int_0^\infty dx\, x J_0(x\alpha r/r_0) \times \exp\left\{-x^2\alpha^2/4\right\} \widetilde{F}_j(x) .$$

The observation region is specified by the distance from the lens to the monochromator, the focus distance of the lens, and the relative hole of the monochromator. To obtain the final quantity which can be compared with the experimentally measured value, one should perform integration exactly over this region:

$$F_j(x_0) = \int_{x_0-\delta}^{x_0+\delta} dx \int_{-\infty}^{\infty} dy\, G(x,y) F_j^t(x,y) ,$$

where x_0 is the displacement of the monochromator from the axis directed from the lens center to the electron-beam center; $G(x,y)$ is the detector function defining the integration domain and the weight of each source of radiation excited by an electron. The detector function $G(x,y)$ has been calculated on the assumption that the lens is ideal.

Figures 3 and 4 show the results of calculations of radiation profiles of the first negative ($\lambda = 391.4$ nm) and the second positive ($\lambda = 337.1$ nm) nitrogen bands as compared to experimental data obtained as the monochromator moved along the electron-beam radius. The electron-beam radius r_0 employed in the calculations has been chosen by the profile of x-ray radiation intensity, assuming that high-energy x-ray photons are generated solely by primary electrons. The calculated excitation rate has been assumed to be proportional to the rate of excitation to the zeroth vibrational level for all energies of electrons.

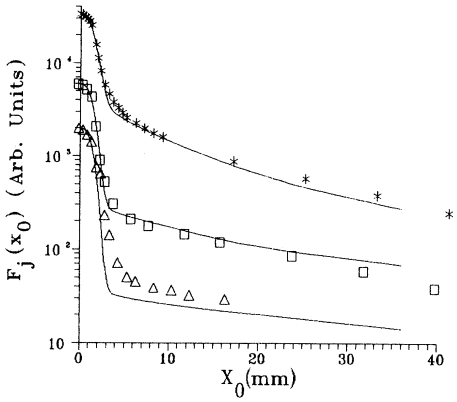

FIG. 3. The radiation profile of the band (00) of the first negative system of nitrogen. Experimental data: $*$, the gas density $n_g = 9 \times 10^{14}$ cm^{-3}, the beam radius $r_0 = 3.2$ mm; $\square$, $n_g = 2.7 \times 10^{14}$ cm^{-3}, $r_0 = 2.6$ mm; $\triangle$, $n_g = 8.7 \times 10^{13}$ cm^{-3}, $r_0 = 2.5$ mm. The solid line represents the calculated excitation rate profile of the state $B\,^2\Sigma_u^+$ in experimental conditions at the corresponding density of nitrogen.

Calculation results represent all peculiarities of experimental findings at different pressures with a good degree of precision. The behavior of secondary electrons is more clearly demonstrated in Fig. 4, which shows the radiation intensities of the band (00) of the second positive system of nitrogen. Since the excitation cross section of the state $C\,^3\Pi_u$ decreases sharply with increasing energy of the exciting electron, radiation of this system is excited by secondary electrons only.

It is to be noted that spatial distribution of secondary electrons is essentially wider than the localized beam

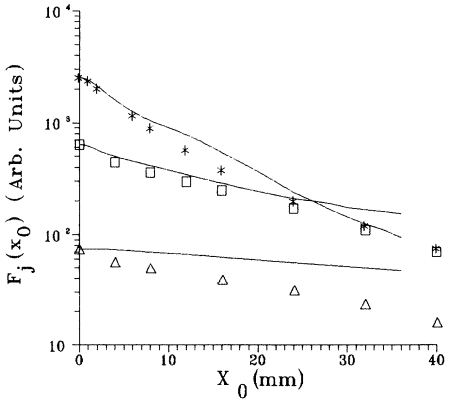

FIG. 4. The radiation profile of the band (00) of the second positive system of nitrogen; conditions and designations same as Fig. 3.

of primary electrons. This result should be taken into consideration during electron-beam measurements and in plasma chemical reactors with electron-beam activation of reactants etc.

Good agreement between theoretical results and experimental evidence in nitrogen allows a definite conclusion on the ability of the above model of the interaction between the electron beam and a gas to adequately represent the spatial energy distribution of electrons in electron-beam plasma, thus the model may also be used for other gas media.

APPENDIX

Taking into account that in cylindrical coordinates

$$|\vec{r} - \vec{r'}| = \sqrt{r^2 + r'^2 - 2rr'\cos(\varphi - \varphi') + (z - z')^2},$$

where r, z are spatial coordinates, the z axis is directed along the electron beam, and φ is the azimuthal angle, we have

$$\frac{\exp\left\{-\sum_k \sigma_t^k n_g^k |\vec{r} - \vec{r'}|\right\}}{|\vec{r} - \vec{r'}|^2} = \int_{\sum_k \sigma_t^k n_g^k}^{\infty} \frac{\exp\{-\beta |\vec{r} - \vec{r'}|\}}{|\vec{r} - \vec{r'}|} d\beta$$
$$= \int_{\sum_k \sigma_t^k n_g^k}^{\infty} d\beta \int_0^{\infty} \frac{dx\, x J_0(xR) \exp\{- \mid z - z' \mid \sqrt{x^2 + \beta^2}\}}{\sqrt{x^2 + \beta^2}},$$

where

$$R = \sqrt{r^2 + r'^2 - 2rr'\cos(\varphi - \varphi')}.$$

Thus Eq. (1) can be written

$$f(r,e) = \frac{\sum_k n_g^k}{2} \int_{-\infty}^{\infty} dz' \int_0^{\infty} dr' r' \int_{\sum_k \sigma_t^k n_g^k}^{\infty} d\beta \int_0^{\infty} dx\, x J_0(rx) J_0(r'x) \frac{\exp(- \mid z - z' \mid \sqrt{x^2 + \beta^2})}{\sqrt{x^2 + \beta^2}}$$
$$\times \left\{ m_e v_b n_b(r') g^k(E,e) \sigma_i^k(E) + \sigma_{\mathrm{el}}^k(e) f(r',e) + \sum_j \sigma_j^k(e + \Delta e_j) f(r', e + \Delta e_j) \right.$$
$$\left. + \int_{e+I_k}^{2e+I_k} d\varepsilon \sigma_i^k(\varepsilon) g^k(\varepsilon, \varepsilon - I_k - e) f(r',\varepsilon) + \int_{2e+I_k}^{(E-I_k)/2} d\varepsilon \sigma_i^k(\varepsilon) g^k(\varepsilon, e) f(r',\varepsilon) \right\}, \tag{A1}$$

where we used the following expression:

$$\int_0^{2\pi} J_0(xR) = \int_0^{2\pi} \left\{ J_0(xr) J_0(xr') + 2 \sum_m J_m(xr) J_m(xr') \cos\{m(\varphi - \varphi')\} \right\} = 2\pi J_0(xr) J_0(xr').$$

By performing the Bessel transformation of Eq. (A1) we can obtain

$$\rho(\nu, e) = \int_0^{\infty} dr\, r J_0(\nu r) f(r,e)$$
$$= \frac{\sum_k n_g^k}{2} \int_{-\infty}^{\infty} dz' \int_0^{\infty} dr\, r J_0(\nu r) \int_0^{\infty} dr' r' \int_{\sum_k \sigma_t^k n_g^k}^{\infty} d\beta \int_0^{\infty} dx\, x J_0(rx) J_0(r'x) \frac{\exp(- \mid z - z' \mid \sqrt{x^2 + \beta^2})}{\sqrt{x^2 + \beta^2}}$$
$$\times \left\{ m_e v_b n_b(r') g^k(E,e) \sigma_i^k(E) + \sigma_{\mathrm{el}}^k(e) f(r',e) + \sum_j \sigma_j^k(e + \Delta e_j) f(r', e + \Delta e_j) \right.$$
$$\left. + \int_{e+I_k}^{2e+I_k} d\varepsilon \sigma_i^k(\varepsilon) g^k(\varepsilon, \varepsilon - I_k - e) f(r',\varepsilon) + \int_{2e+I_k}^{(E-I_k)/2} d\varepsilon \sigma_i^k(\varepsilon) g^k(\varepsilon, e) f(r',\varepsilon) \right\}$$

$$= \frac{\sum_k n_g^k}{2} \int_{-\infty}^{\infty} dz' \int_{\sum_k \sigma_t^k n_g^k}^{\infty} d\beta \frac{\exp(-\mid z - z' \mid \sqrt{x^2+\beta^2})}{\sqrt{x^2+\beta^2}}$$

$$\times \left\{ m_e v_b \omega(\nu) g^k(E,e) \sigma_i^k(E) + \sigma_{\rm el}^k(e)\rho(\nu,e) + \sum_j \sigma_j^k(e+\Delta e_j)\rho(r', e+\Delta e_j) \right.$$

$$\left. + \int_{e+I_k}^{2e+I_k} d\varepsilon \sigma_i^k(\varepsilon) g^k(\varepsilon, \varepsilon - I_k - e)\rho(\nu,\varepsilon) + \int_{2e+I_k}^{(E-I_k)/2} d\varepsilon \sigma_i^k(\varepsilon) g^k(\varepsilon,e)\rho(\nu,\varepsilon) \right\}, \quad \text{(A2)}$$

where we used

$$\int_0^{\infty} dr r J_0(\nu r) J_0(xr) = \frac{1}{\nu}\delta(\nu - x).$$

Taking into account that

$$\int_{-\infty}^{\infty} dz' \int_{\sum_k \sigma_t^k n_g^k}^{\infty} d\beta \frac{\exp(-\mid z - z' \mid \sqrt{x^2+\beta^2})}{\sqrt{x^2+\beta^2}} = 2 \int_{\sum_k \sigma_t^k n_g^k}^{\infty} \frac{d\beta}{\nu^2+\beta^2} = \frac{2}{\nu} \arctan \frac{\nu}{\sum_k \sigma_t^k n_g^k},$$

we obtained Eq. (2).

[1] C. H. Jackman and A. E. S. Green, J. Geophys. Res. **84**, 2715 (1979), and references therein.

[2] V. P. Konovalov and E. E. Son, in *Plasma Chemistry*, edited by B. M. Smirnov (Energoatomizdat, Moscow, 1987), Vol. 14, p. 194, and references therein.

[3] H. Itoh, M. Shimozuma, and H. Tagashira, J. Phys. D **13**, 1201 (1980); H. Itoh, Y. Miura, N. Ikuta, Y. Nakano, and H. Tagashira, *ibid.* **21**, 922 (1988); Y. Ohmori, M. Shimozuma, and H. Tagashira, *ibid.* **21**, 724 (1988); P. J. Drallos and J. M. Wadehra, Phys. Rev. A **40**, 1967 (1989); H. Date, K. Kondo, and H. Tagashira, J. Phys. D **26**, 1211 (1993).

[4] J. Bretagne, G. Delonya, J. Godart, and V. Puech, J. Phys. D **14**, 1225 (1981); J. Bretagne, J. Godart, and V. Puech, *ibid.* **15**, 2205 (1982).

[5] M. G. Heaps and A. E. S. Green, J. Appl. Phys. **45**, 3183 (1974); M. J. Berger, S. M. Seltzer, and K. Maeda, J. Atmos. Terr. Phys. **26**, 591 (1974); Dayashankar, S. T. Suh, and A. E. S. Green, Int. J. Quantum Chem. **20**, 547 (1986); G. J. Kutcher and A. E. S. Green, J. Appl. Phys. **47**, 547 (1986).

[6] Z. Yu, Z. Luo, T. Y. Sheng, H. Zarnani, C. Lin, and G. J. Collins, IEEE Trans. Plasma Sci. **18**, 753 (1990).

[7] A. K. Rebrov, G. I. Sukhinin, R. G. Scharafutdinov, and J. C. Lengrand, Zh. Tekh. Fiz. **51**, 1832 (1981) [Sov. Phys. Tech. Phys. **26**, 1062 (1981)].

[8] K. M. Case and P. F. Zweifel, *Linear Transport Theory* (Addison-Wesley, Ontario, 1967), p. 384.

[9] J. P. Boeuf and E. Marode, J. Phys. D **15**, 2169 (1982); K. Satoh, H. Itoh, Y. Nakano, and H. Tagashira, *ibid.* **21**, 931 (1988); M. Yumoto, Y. Kuroda, and T. Sakai, *ibid.* **24**, 1594 (1991); J. Liu and G. R. G. Raju, *ibid.* **25**, 167 (1992); M. S. Dincer, *ibid.* **26**, 1427 (1993); J. W. Keto, J. Chem. Phys. **74**, 4445 (1981).

[10] D. Rapp and P. Englander-Golden, J. Chem. Phys. **43**, 1464 (1965).

[11] D. C. Cartwright, S. Trajmar, A. Clutjian, and W. Williams, Phys. Rev. A **16**, 1041 (1977).

[12] J. Itikawa *et al.*, J. Phys. Chem. Ref. Data **15**, 985 (1986).

[13] C. B. Opal, W. K. Peterson, and E. C. Beaty, J. Chem. Phys. **55**, 4100 (1972).

[14] Complete description of the experimental setup can be found in B. N. Borsenko, N. V. Karelov, A. K. Rebrov, and R. G. Scharafutdinov, Zh. Prikl. Meck. Tekh. Fiz. **5**, 20 (1976) [J. Appl. Mech. Tech. Phys. (USSR) **17**, 615 (1976)].